

## **A DUAL BAND CIRCULARLY POLARIZED RING ANTENNA BASED ON COMPOSITE RIGHT AND LEFT HANDED METAMATERIALS**

**A. Yu, F. Yang, and A. Elsherbeni**

Center of Applied Electromagnetic Systems Research (CAESR)  
Department of Electrical Engineering  
The University of Mississippi  
University, MS 38677, USA

**Abstract**—In this paper a dual band circularly polarized antenna is designed, fabricated, and measured. Based on the concept of composite right and left handed (CRLH) metamaterials, the same phase constants and current distributions on the ring antenna are achieved at two frequency bands. Thus, the antenna has similar radiation patterns at both bands. The circular polarization is implemented by feeding two vertical ports from power dividers that provide equal magnitudes and quadrature phase excitations.

### **1. INTRODUCTION**

Dual band circularly polarized antennas have been realized by a variety of structures. By using stacked microstrip patches [1–4] or a single patch [5,6], multiple resonances can be obtained. Reconfigurable antennas with MEMS switches [7] and pin diodes [8] have also been studied for dual band CP operation. However, these structures usually generate different radiation patterns in the dual bands due to different current distributions.

Recently, the left handed metamaterial and the composite right and left handed (CRLH) metamaterials were proposed and applied for enhancing antenna designs [9–18]. They are basically the dual of traditional transmission lines. Series inter-digital capacitors and shunt stub inductors are introduced in a microstrip transmission line, as illustrated in Fig. 1. The dispersion relation of a CRLH is characterized

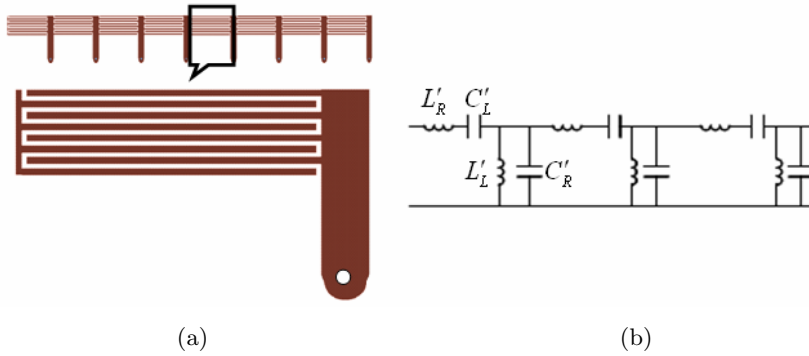


**Figure 1.** Composite right left handed (CRLH) transmission line: (a) structure and (b) circuit model.

by a nonlinear equation [9]:

$$\beta = \omega \sqrt{L'_R C'_R} - \frac{1}{\omega \sqrt{L'_L C'_L}} \quad (1)$$

where  $\beta$  is the propagation constant,  $\omega$  is the angular frequency, and  $L'_R, C'_R, L'_L, C'_L$  are characteristic inductances and capacitances of the CRLH transmission line shown in Fig. 1(b). The metamaterial transmission line allows the existence of backward waves, in other words, negative propagation constants. Thus, two different frequencies can have the same propagation constant (in the sense of absolute value) through this dispersion relation. As a consequence, the same mode and current distribution are achieved in the two different frequency bands. This property is utilized in this paper to design a dual band ring antenna with the same circularly polarized pattern.

## 2. PRINCIPLE AND CONFIGURATION OF THE ANTENNA

A CRLH transmission line can be realized by periodical microstrip structures. The unit cell is the combination of a series of inter-digital capacitor and a shunt stub inductor, as depicted in Fig. 1. To design a ring antenna, the CRLH transmission line is bent into a circle, as shown in Fig. 2(a). When the circumference  $L$  of a loop resonator is equal to one wavelength  $\lambda$ ,  $L = \lambda$ , the loop resonates at the basic mode with the corresponding frequency.

Now for a fixed circumference  $L$ , suppose a resonant frequency  $f_1$  is specified, and the loop resonates at the basic mode. From Equation

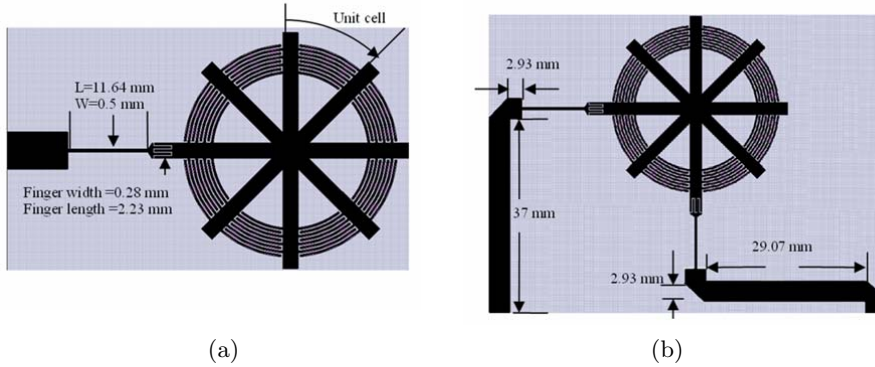


**Figure 2.** Antenna configuration (with the ground plane 76 mm by 71 mm).

(1), a relationship is established for the four design parameters  $L'_R$ ,  $C'_R$ ,  $L'_L$ , and  $C'_L$ :

$$\beta_1 = \frac{2\pi}{L} = \omega_1 \sqrt{L'_R C'_R} - \frac{1}{\omega_1 \sqrt{L'_L C'_L}}. \quad (2)$$

The consideration of matching yields another two equations:

$$\sqrt{\frac{L'_R}{C'_R}} = Z_c \quad (3)$$

$$\sqrt{\frac{L'_L}{C'_L}} = Z_c \quad (4)$$

where  $Z_c$  is the characteristic impedance of the feeding line. Therefore, still another freedom is left for the determination of the four design parameters. In order to have the ring resonate at another frequency  $f_2$ , the fourth restriction can be written as following based on the negative propagation constant of the CRLH transmission line:

$$\beta_2 = -\frac{2\pi}{L} = \omega_2 \sqrt{L'_R C'_R} - \frac{1}{\omega_2 \sqrt{L'_L C'_L}} \quad (5)$$

The minus sign indicates that the CRLH transmission line is supporting a backward wave at the second frequency  $f_2$ . It's clear that the propagation constants at these two frequencies have the opposite signs but the same absolute values. Thus, the current distributions at these two frequencies are the same.

Using this concept, the antenna is built with 8 unit cells of the CRLH transmission line, as shown in Fig. 2(a), where the shunt inductances are basically shorting stubs. The ends of the stubs are connected together, forming a virtual ground. The dimensions of the CRLH line are designed to obtain the characteristic parameters  $L'_R$ ,  $C'_R$ ,  $L'_L$ , and  $C'_L$  for dual band operation. Detailed design procedure of a CRLH line can be found in [9].

The matching system of the antenna is composed of a coupling inter-digital capacitor, a section of high impedance microstrip line and a traditional  $50\ \Omega$  microstrip line. In concern of fabrication, the antenna and the feeding system have different parameters than [10]. It is found that the characteristic impedance of the matching line plays a critical role in tuning the match at both frequencies.

Next, the circular polarization in dual bands is realized by exciting the antenna at two perpendicular ports, as depicted in Fig. 2(b). For the sake of convenient tuning and assembling, two  $50\ \Omega$  transmission lines with the same length are added in order to bring the feeding ports to the same side of the circuit board. Power dividers are then designed to provide  $90^\circ$  phase shift and connected to these two feeding ports through SMA connectors.

### 3. SIMULATION AND MEASUREMENT RESULTS

The antenna and the power dividers with finite ground planes are modeled using Advanced Design System (ADS) Momentum. The outermost radius of the ring is 13.8 mm, with the length of 15.3 mm for each spike. The finger width of the inter-digital capacitor is 0.35 mm, while the slot width is 0.15 mm [11]. The other dimensions are provided in Fig. 2, where (a) shows the ring and the matching system and (b) gives the entire view with two  $50\ \Omega$  feeding lines, with the widths of 4.78 mm. The antenna is built on RT/Duroid 5880 substrate, with relative permittivity of 2.2 and thickness of 1.57 mm.

Simulated results of the antenna in Fig. 2(b) are shown in Figs. 3 and 4. It is observed that the return loss of the two ports,  $S_{11}$  and  $S_{22}$ , exhibit almost the same resonant behavior, which demonstrates that the two modes excited at each port are independent of each other. The radiation patterns at two frequency bands are also alike, except that the cross-polarization within the upper band is somewhat higher than that in the lower band. This can be explained as the radiation at the discontinuities along the feed line, which is stronger at higher frequencies.

Figures 5(a) and 5(b) present photos of the fabricated antenna sample and power dividers. The power dividers are built on RT/Duroid

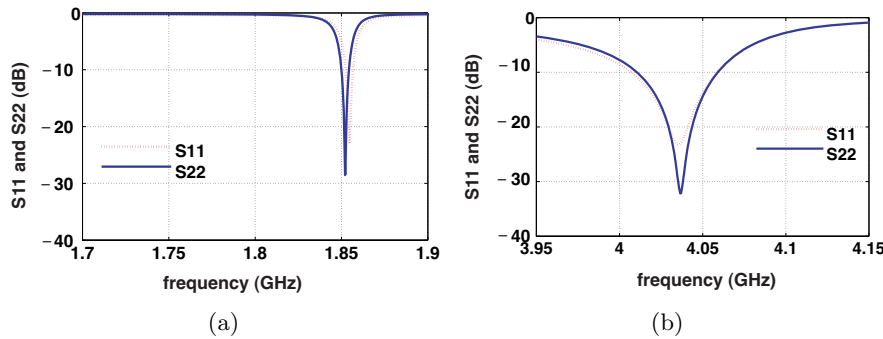


**Figure 3.** Computed return losses at (a) the lower band and (b) the upper band.

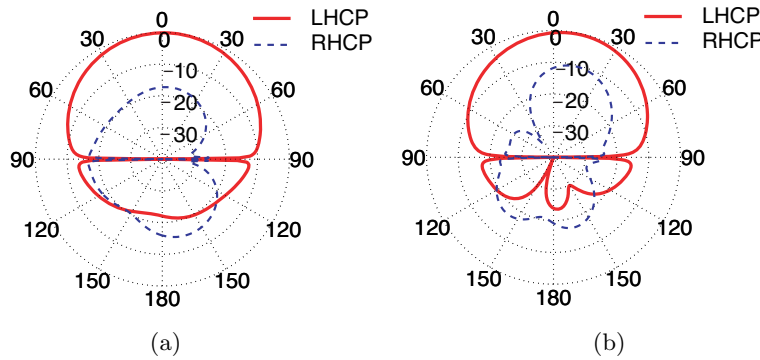


**Figure 4.** Computed radiations pattern in  $X-Z$  plane at (a) the lower band and (b) the upper band.

5880 substrate, with relative permittivity of 2.2 and thickness of 0.785 mm. The return loss of the complete antenna with power dividers is measured and the results are plotted in Fig. 6. The antenna has its dual band located at the frequency ranges of 1.768~1.776 GHz and 3.868~4.007 GHz, namely, 0.5% and 3.6% impedance bandwidth in the lower and upper bands, respectively. The measured frequency is slightly lower than the simulation results, which may results from the incorporation of the power dividers.

The frequency response of axial ratios measured at the broadside direction is demonstrated in Fig. 7. The minimum axial ratios are located at 1.778 GHz and 3.97 GHz. Figure 8 illustrates the spinning linear patterns at these two frequencies. The pattern at the higher frequency is somewhat oblique due to the relatively high cross

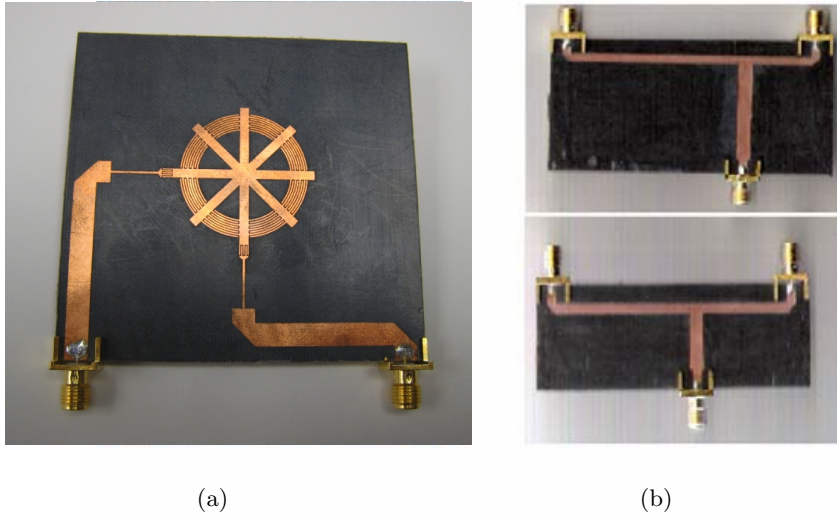


**Figure 5.** (a) Picture of the fabricated antenna with adapters, (b) power dividers for the lower band (top) and the upper band (bottom).

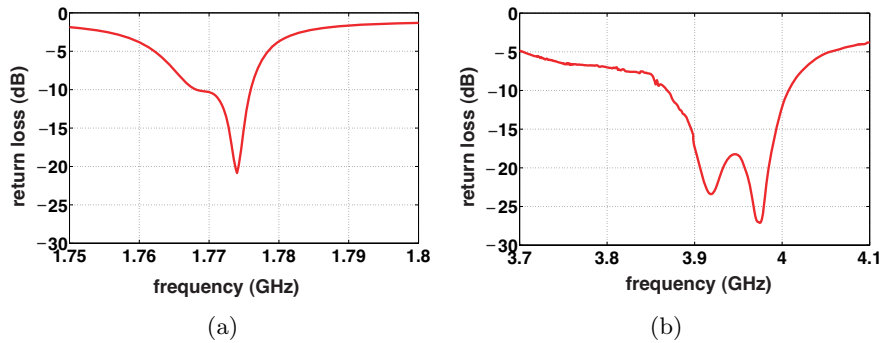


**Figure 6.** Measured return losses at (a) the lower band and (b) the upper band.

polarization, which has been observed in Fig. 4. Basically, the patterns at both frequencies are with the broadside feature and have their beam widths (around  $70^\circ$  for 3 dB) close to each other. Finally, the antenna gain within the dual bands is measured and the peak gains reach 2.5 dB for both of the frequency ranges.

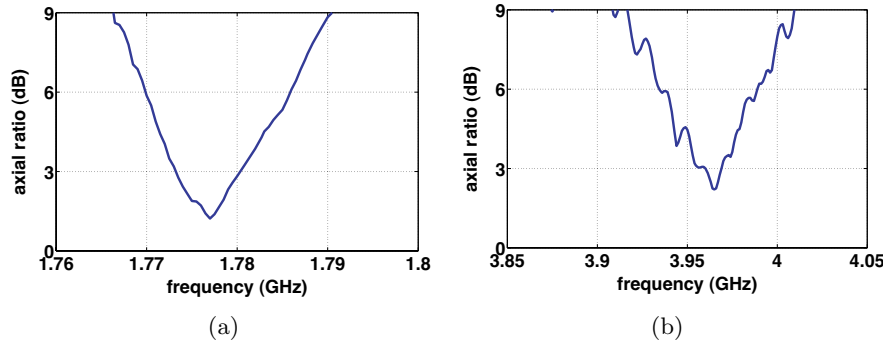


**Figure 7.** Measured axial ratio frequency response in the broadside direction at (a) the lower band and (b) the upper band.

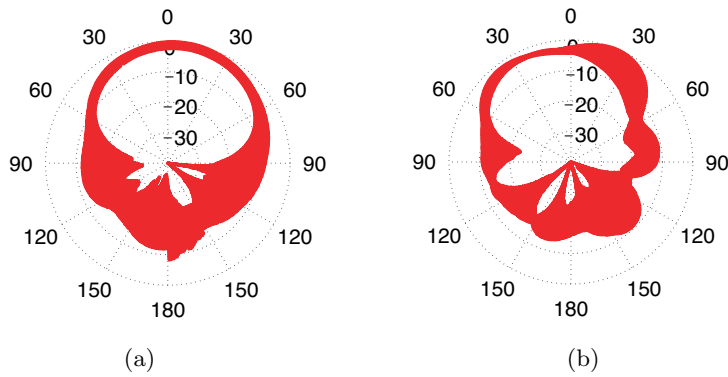


**Figure 8.** Measured spinning patterns in  $X-Z$  plane at (a) the lower band and (b) the upper band.

#### 4. CONCLUSION

A circularly polarized dual band antenna based on the concept of CRLH transmission line has been realized, with two separated power dividers providing  $90^\circ$  phase shift between the two input ports. The antenna operates at 1.778 GHz and 3.97 GHz with good axial ratios. The co-polarized radiation patterns within the dual bands are basically the same while a relatively high cross polarization level is observed at the higher frequency due to the radiation at the discontinuities along the feed line.

## REFERENCES

1. Jan, J. Y. and K. L. Wong, "A dual band circularly polarized stacked elliptic microstrip antenna," *Microwave and Optical Technology Letters*, Vol. 24, No. 5, 354–357, March 2000.
2. Lau, K. L. and K. M. Luk, "A wide band circularly polarized L-probe coupled patch antenna for dual band operation," *IEEE Transactions on Antennas and Propagation*, Vol. 53, No. 8, 2636–2644, August 2005.
3. Su, C. W., C. M. Su, and K. L. Wong, "Compact dual band circularly polarized antenna for GPS/ETC operation on vehicles," *Microwave and Optical Technology Letters*, Vol. 40, No. 6, 509–511, March 2004.
4. Sudha, T. and T. S. Vedevalthy, "A dual band circularly polarized microstrip antenna on an EBG substrate," *IEEE AP-Symposium Digest*, 68–71, 2002.
5. Avitabile, G., S. Maci, F. Bonifacio, and G. Salvador, "Dual band circularly polarized patch antenna," *IEEE AP-Symposium Digest*, 290–293, 1994.
6. Liu, Z. D., P. S. Hall, and D. Wake, "Dual frequency planar circularly polarized antenna at S and L bands," *Tenth International Conference on Antennas and Propagation*, 14–17, April 1997.
7. Jung, C., M. Lee, S. Liu, G. P. Li, and F. D. Flaviis, "Reconfigurable patch antenna for frequency diversity with high frequency ratio (1.6:1)," *International Telemetry Conference*, 24–27, October 2005.
8. Yang, F. and Y. Rahmat-Samii, "A reconfigurable patch antenna using switchable slots for circular polarization diversity," *Microwave and Wireless Component Letters*, Vol. 12, Issue 3, 96–98, March 2002.
9. Caloz, C. and T. Itoh, *Electromagnetic Metamaterials, Transmission Line Theory and Microwave Applications*, Wiley, New York, 2006.
10. Otto, S., A. Rennings, C. Caloz, P. Waldow, and T. Itoh, "Composite right/left-handed  $\lambda$ -resonator ring antenna for dual frequency operation," *IEEE AP-Symposium Digest*, 684–687, Washington, DC, 2005.
11. Yang, R., Y. Xie, P. Wang, and T. Yang, "Conjugate left- and right-handed material bilayered substrates qualify the subwavelength cavity resonator microstrip antennas as sensors," *J. of Electromagn. Waves and Appl.*, Vol. 20, No. 15, 2113–2122,

- 2006.
12. Chen, H., B.-I. Wu, and J. A. Kong, "Review of electromagnetic theory in left-handed materials," *J. of Electromagn. Waves and Appl.*, Vol. 20, No. 15, 2137–2151, 2006.
  13. Grzegorzcyk, T. M. and J. A. Kong, "Review of left-handed metamaterials: evolution from theoretical and numerical studies to potential applications," *J. of Electromagn. Waves and Appl.*, Vol. 20, No. 14, 2053–2064, 2006.
  14. Yang, R., Y. Xie, P. Wang, and L. Li, "Microstrip antennas with left-handed materials substrates," *J. of Electromagn. Waves and Appl.*, Vol. 20, No. 9, 1221–1233, 2006.
  15. Xu, W., L.-W. Li, H.-Y. Yao, and T.-S. Yeo, "Left-handed material effects on waves modes and resonant frequencies: filled waveguide structures and substrate-loaded patch antennas," *J. of Electromagn. Waves and Appl.*, Vol. 19, No. 15, 2033–2047, 2005.
  16. Wu, B.-I., W. Wang, J. Pacheco, X. Chen, T. Grzegorzcyk, and J. A. Kong, "A study of using metamaterials as antenna substrate to enhance gain," *Progress In Electromagnetics Research*, PIER 51, 295–328, 2005.
  17. Sui, Q., C. Li, L. L. Li, and F. Li, "Experimental study of  $\lambda/4$  monopole antennas in a left-handed meta-material," *Progress In Electromagnetics Research*, PIER 51, 281–293, 2005.
  18. Semichaevsky, A. and A. Akyurtlu, "Homogenization of metamaterial-loaded substrates and superstrates for antennas," *Progress In Electromagnetics Research*, PIER 71, 129–147, 2005.
  19. Yu, A., F. Yang, and A. Elsherbeni, "Circularly polarized dual band ring antenna using composite right and left handed metamaterial," *The First European Conference on Antennas and Propagation*, 532–536, November 2006.